Investigating a novel nanoneedle-based technology for assessment of AAV product quality and manufacturing performance

Daniel Hurwit, Douglas Steinhauff, **Bristol Myers Squibb**

Angad Garg, Tal Raz, Qimin Quan, **NanoMosaic Inc**

Highlights

- A novel, multi-omic nanoneedle technology has been used to quantify heterogenous sub-populations of AAV across a range of different matrices and manufacturing processes.
- The genomic titer of the intact, full-length transgene (3.3kb) is compared to that of truncated species, highlighting disadvantages and limitations of some common approaches such as ITR-based tittering where quantification requires caution in selecting standards and interpreting the data.
- Several new or lesser-discussed attributes of interest and potential targets of process optimization are presented, including the ability to independently identify left *vs.* right truncation events with a process-development-friendly analytical tool, and relevant approaches to interpret them in relation to other species.
- The nanoneedle technology presents an attractive approach for quantifying the true full-length transgene of interest and identifying pools of partials that can persist in AAV feed streams throughout the manufacturing process.
- The ratio of full-length *vs.* total packaged viral genome species is proposed as a measure for assessing AAV product quality and manufacturing performance in an effort to emphasize the impact of packaged truncated species and distinguish from the typical % full measurement.

Introduction

Adeno-associated virus (AAV) gene therapy is an innovative approach aimed at treating genetic disorders by delivering therapeutic genes to targeted cells. AAVs are small, non-pathogenic, minimally integrating viruses, making them ideal vectors for gene therapy. AAVs are generally considered safe, as they minimally integrate into the host genome and are generally well tolerated. They also offer serotype-specific tropism, where targeting of specific tissues allows for more precise treatment of diseases. Once delivered, the therapeutic genes can persist in cells for extended periods, potentially providing long-term benefits with a single administration, especially when targeted against non-dividing cells. AAVs are also the vector of choice for *ex vivo* gene edited cell

therapies, transducing T cells with high efficiency for use as templates for gene integration pathways such as homology directed repair. To date there have been eight approved AAV gene therapies; however, hundreds more gene and cell therapies leveraging Adeno-associated viral vectors are progressing through the clinic [1].

One of the greatest challenges in AAV gene therapy is the development of manufacturing processes that yield high quality vector at low cost [2]. While great progress has been made improving and intensifying processes towards better quality and lower COGM (cost of goods manufactured), including - scaling up processes, increasing productivity and yield, simplifying operations, and leveraging increasing understanding of CQAs - there is still much to be desired. Even for highly productive processes that appear to yield high percent full vector substance (e.g. >90% in some cases), particle-to-infectivity (P:I) ratios for recombinant AAV can vary from 10:1 to 10,000:1 with ratios on the order of 1000:1 being fairly common [3]. P:I is a critical measure of AAV quality and anything above 1:1 suggests some amount of defective viral particles. At 1000:1, production of 999 defective parts out of every thousand is a difficult business model for manufacturing. This is true regardless of use case, though may be readily exemplified in the case of high-dose systemic therapies to adult patient populations. These can end up costing hundreds-of-thousands to several million dollars per dose. Additionally, high-dose therapies could pose potential safety risks to patients where an immune response may trigger severe inflammation and liver toxicity and/or limit the efficacy of the treatment [4].

Unfortunately, there remains a significant knowledge gap when it comes to characterizing non-functional AAV particles. When comparing recombinant AAV to wild-type, which can often have a particle-to-infectivity ratio of 1 (every particle is capable of infecting a hose cell) [5], there are still many etiological unknowns behind the difference. While not yet proven to explain the functional differences between recombinant and wild-type AAV, one noteworthy difference is in the composition of the packaged genetic material. Whereas wild type AAV is considered to package mostly full-length vector genomes, recombinant AAV (rAAV) comes in an extremely heterogenous population where “true full” vector genomes are often the minority, perhaps more so than current analytical methods reveal [6]. Thus, one of the greatest opportunities in the field of AAV gene therapy remains meaningfully increasing the proportion of true full-length packaged vector genomes, both out of the bioreactor as well as after purification. Development of operations towards these aims, and the ability to test and validate their impact, is challenging and necessitates new analytics that quantify the correct vector attribute and have sufficient throughput.

Current tittering methods include both biophysical (e.g. DLS, SEC-MALS, RP-HPLC, Mass Photometry, Analytical Ultracentrifugation, etc.) and molecular approaches (e.g. digital droplet PCR (ddPCR) and quantitative PCR (qPCR)) [6]. Biophysical methods are generally simple but are limited in their ability to confirm identity or distinguish subpopulations of AAV particles with any real granularity, and usually require clean and concentrated feed-streams. Molecular methods can be powerful but are prone to variability and can be quantitatively biased by primer/probe design. While these methods have specific applications, they fall short in providing an accurate quantitation of true full-length vector genome containing particles, as well as a detailed quantitative analysis of various populations of particles containing partial genomes.

The NanoMosaic Tessie platform, based on a novel nanoneedle technology, quantifies any region of DNA of interest without limitation of size across the AAV genome and is proposed as a means of overcoming some of these limitations. The full-length NanoMosaic assay is designed to quantify the entire full-length transgene accounting for the 'therapeutic genome' and determine its titer accurately and specifically.

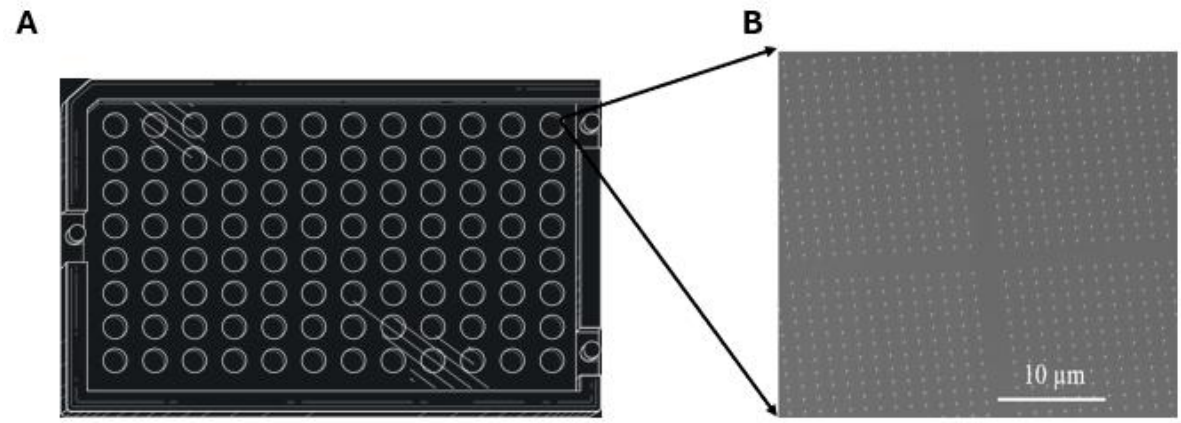

Fig. 1. Nano-plate consumable. A. SBS 96-format nano-plate and nanoneedles. **B.** Scanning electron microscope image of the nanoneedles.

Method

The detection of biomolecules is conventionally achieved through labeling the analytes with reporters that have large fluorescence or absorption signatures. This is typically not compatible to wide-field, high-throughput imaging, as it requires high-intensity light sources, long integration times and optical components with high magnifications and large numerical apertures. The reporters are also not universally compatible with complex sample matrices, as blinking and bleaching properties will increase the variance in the detection signal. The nanoneedle technology is developed to use a solid-state nanostructure to replace the need for molecular reporters. Light scattered from the nanoneedle responds sensitively to the changes of local refractive index at the surface of the nanoneedle. Therefore, when molecules bind to the nanoneedles, the scattering spectrum will shift in response to the increases in local refractive index and can be used to quantify the number of analyte molecules in the sample.

In the nano-plate consumable, the nanoneedles are densely and integrally arrayed on a silicon chip (**Fig. 1**). Using dark-field microscopy, a sensor that consists of >20,000 nanoneedles is imaged in a single exposure with a CMOS (Complementary Metal-Oxide-Semiconductor) color camera. The nano-plate consumable is formatted in accordance with the Society for Biomolecular Screening (SBS) format to be easily used with standard liquid handling systems for automation. More than 2 billion total nanoneedles can be integrated on to a standard SBS plate, which can be configured into 96, 384 or 1536 well format for high throughput workflows.

The nanoneedle assay workflow is illustrated in **Fig. 2**. A sample volume of 2 µL is required. Standard sample preparation processes are used to lyse viral particles and release the transgene (**Fig. 2, top panel**). The assay utilizes plasmid DNA as a standard.

The inverted terminal repeats flanking the transgene are the critical sequences of the viral genome required for replication and packaging, yet they pose significant challenges in accurately determining titers (detailed in the final section). Thus, as shown in **Fig. 2, top panel,** the ITRs are removed from the released transgene by restriction digestion of the double-stranded ITR-A-region (BssHII enzyme). Alternative enzymes close to the 5' and 3' ends of the transgene can also be used if the BssHII restriction enzyme is incompatible with the transgene sequence. To measure the ITR molecules specifically, restriction digestion steps can be omitted and the guidelines detailed in the last section can be followed.

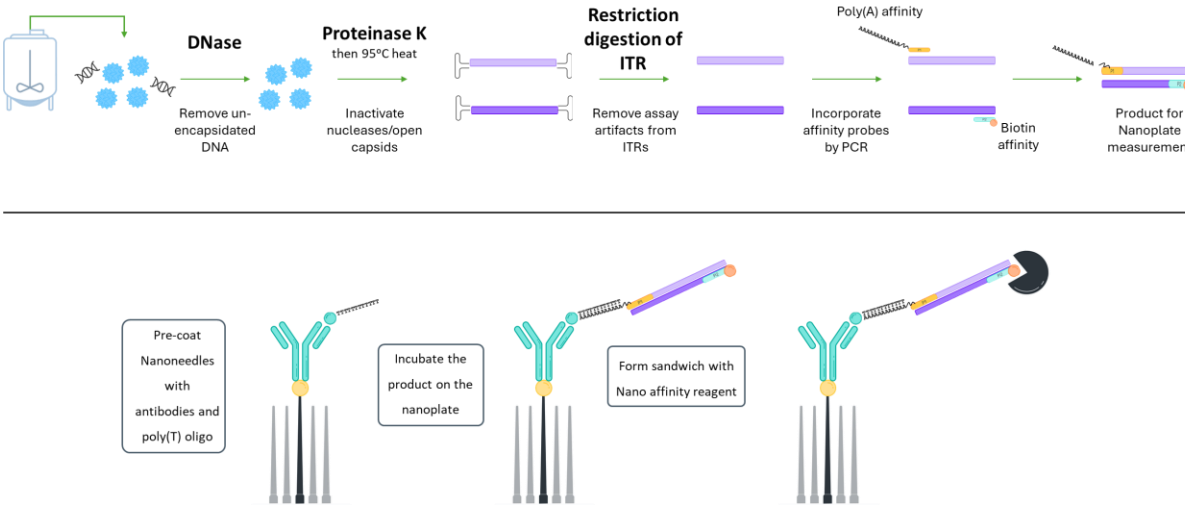

Fig. 2. Viral genome assay workflow. Top panel (sample preparation): Transgene is released from the sample using standard sample preparation methods and ITRs are removed by restriction digestion. The sample is then mixed with two oligonucleotide probes with sequences specifically matching the two ends of the transgene region of interest. The poly(A) and biotin affinity tags are incorporated into a double-stranded DNA product using the viral genome as template with a few cycles of PCR. **Bottom panel (nanoplate workflow):** A nanoplate is coated with antibodies containing poly(T) tags, allowing the product generated to be captured on the nanoneedle. The nano-affinity reagent further binds to the biotin, inducing an enhanced scattering spectrum change quantified by the NanoMosaic Tessie reader.

Viral genome titers are measured using a standard curve created with the vector plasmid (digested with the same restriction enzymes as the sample). Two oligonucleotide probes (P1 and P2) with affinity tags [poly(A) for P1, biotin for P2] are added to the sample and standards after restriction digestion. The affinity tags are incorporated into a double-stranded DNA product after a few PCR cycles (**Fig. 2, top panel**). The positions of the probes will determine the transgene sub-population to be quantified. For example, for full-length transgene (defined as the therapeutic region containing the full DNA with the target transgene and all regulatory regions), probes should be positioned at

opposite ends of the transgene. Probes for truncated transgene titers should span the region of interest (e.g., areas where truncations are suspected).

During sample preparation, no DNA purification is required, and all steps are performed in the same tube ensuring: (i) no loss of DNA due to sample clean-up, volume exchanges or tube adherence, thus maximizing sample preparation efficiency, and (ii) assay compatibility with high-throughput automation.

A nano-plate is prepared by coating the surface with an antibody attached to a modified poly(T)-oligo (**Fig. 2, bottom panel**). After incubating the prepared DNA product (shown in **Fig. 2 top panel**) on the nanoplate, the targeted transgene population is captured by the nanoneedles via hybridization of the poly(A) tag to the poly(T) oligonucleotide, as shown in **Fig. 2, bottom panel**. Last, the biotin tag at the other end of the DNA product binds to the nano-affinity reagent (**Fig. 2, bottom panel**), inducing an enhanced light scattering spectrum change of the nanoneedle, above the threshold set by the analysis algorithm. This ensures that the only molecules that are detected have both affinity tags incorporated into the amplified product. For example, in case of the full-length transgene, only when the double stranded product has formed, will a signal be generated on the nanoneedles. The nanoplate is then analyzed by the NanoMosaic Tessie reader.

The nanoneedle full-length assay is easy to implement and allows for further verification by measuring the product size of the amplified product (e.g., as shown in **Fig. 4C**). The closest comparison to the current full-length assay would be one of the various types of "linkage assays", such as 2-color ddPCR, which measures the coexistence of two fragments in the same droplet.

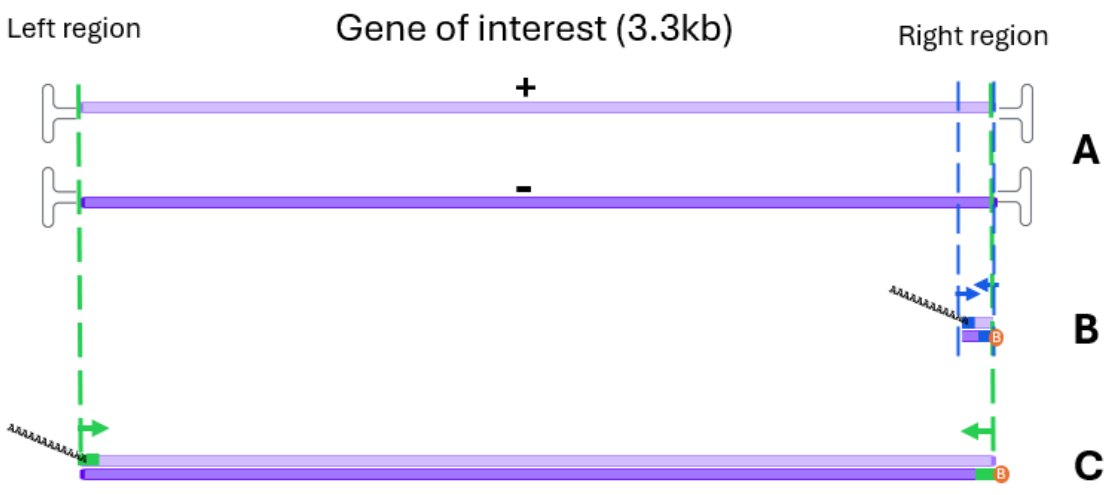

Fig. 3. AAV construct and probe design. A. AAV construct in this study has a 3.3kb transgene size. **B.** The probe set against the right-end of the transgene is shown in blue arrows. Right-end probes will bind to any overlapping transgene molecules including any left truncated molecules and the full-length transgene. **C.** The probe set against the full-length transgene is shown in green arrows. This probe-set measures only the full-length transgene and not any truncations since both ends of the transgene are required for detection.

However, 2-color ddPCR cannot distinguish between intact full-length molecules *vs* those with internal deletions, nor can it differentiate between true linked fragments *vs* mere co-existence of two fragments (which may result from overpacking of small fragment within one viral vector). In addition, optimizing the 2-color assay for two sets of primers and probes can be challenging, often requiring compromises in selecting which two fragments can be co-measured under the same assay condition.

For our study, we developed two transgene assays probing a short region at the right terminus of the transgene and the full-length region. The positions of the probes and their resulting products for the short and full-length regions are shown in **Fig. 3B** and **3C**, respectively. In **Table 1**, we further summarize the probe annealing region and amplified product for short-region and full-length assays, respectively, for typical heterogeneous species in rAAV preparations [7].

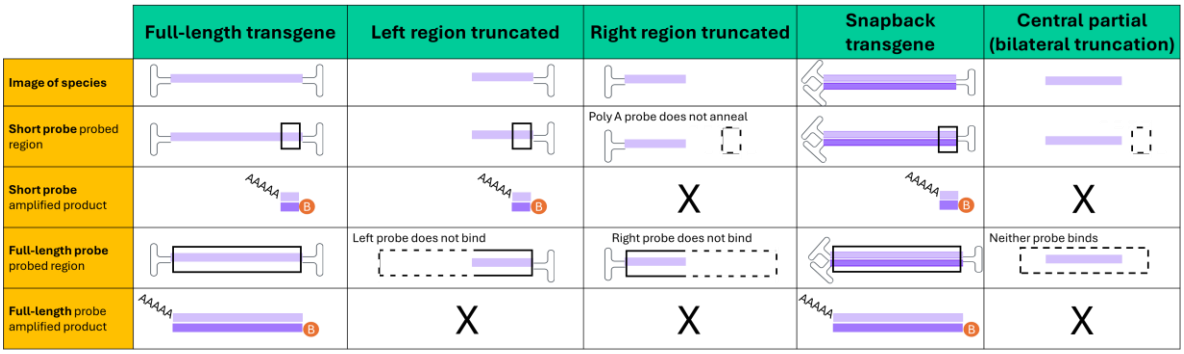

Table 1: Examples of different species in the rAAV sample. The boxed region shows the area to be amplified, either for the short or the full-length regions, with the two affinity probes binding at each end. The amplified product bearing the affinities is shown in cases where both the probes can anneal.

Results

AAV samples from two manufacturing processes

AAV produced by two different manufacturing processes was evaluated. Both processes employ triple transient transfection of HEK293 cells in suspension, though each process leverages a HEK293 cell line. For both processes, cells were harvested 3 days post-transfection, lysed, and clarified by depth filtration. In one of the processes the vector was then concentrated by tangential flow filtration (TFF1) followed by affinity chromatography (AC), virus retentive filtration (VRF), another round of TFF (TFF2), and finally sterilizing-grade filtration. In the other process, the clarified harvest was loaded directly on AC, then enriched via anion exchange chromatography (AEX), followed by VRF, TFF2, and final sterilizing grade filtration. These are described as “Process A” and “Process B”, respectively.

Full-length and short-region viral genome assays and quantification of in-process samples

We tested samples from different stages of manufacturing, quantifying two regions for measuring the viral genome (VG) titer: a short 116-nucleotide right-ITR-adjacent region of the transgene (**Fig. 3B**), and the full-length (FL) transgene that reflects the therapeutic dose as shown in (**Fig. 3C**).

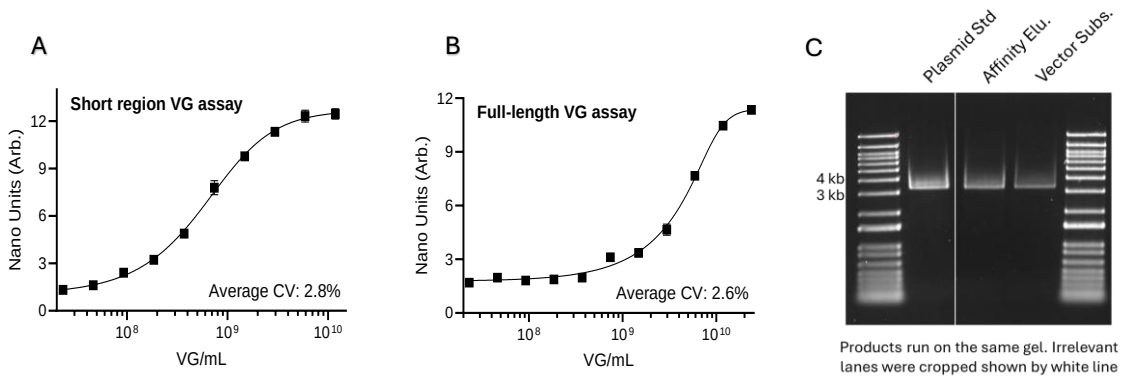

Fig. 4. Assay Qualification. Calibration curves for the (**A**) short region and (**B**) full-length (FL) VG assays and average CV of the standards are 2.8% and 2.6%, respectively. **C.** Agarose gel analysis of the product after probe incorporation shows a single band at the expected full-length size.

To determine the short-region and full-length genome titers, we first developed the assay parameters by evaluating the dynamic range and variability using restriction digested plasmid as standard. The probe incorporation was conducted for 12 cycles both for the short and FL regions. The dynamic ranges are 1E+08 – 3E+10 VG/mL and 1E+09 – 3E+10 VG/mL, respectively for short and FL regions (**Fig. 4 A & B**). The average variabilities (CV) are 2.8% and 2.6%, respectively. The full-length assay specificity was confirmed by measuring the size of the product from the standard as well as the two samples from the manufacturing batch (**Fig. 4C**) by agarose gel electrophoresis.

Samples from the two different manufacturing runs were quantified using the short and the full-length regions. The samples evaluated for Process A were crude lysate, TFF1 pool, VRF load, and vector product. The samples evaluated for Process B were crude lysate, affinity elution pool, AEX elution pool (AEX eluate), and vector substance. The quantification from the short and the full-length region is shown in **Fig. 5 and Table 2**. Each sample was run in six dilutions, with technical replicates for each dilution. Dilution results were discarded if they fell out of the linear range of the standard curve. The linearity CV, a measure calculated from the standard deviations of the average recovery measurements from multiple dilutions, indicates any potential matrix interference. Although the CVs suggest room for additional method development, without optimization, they are on par with other molecular tittering methods like qPCR.

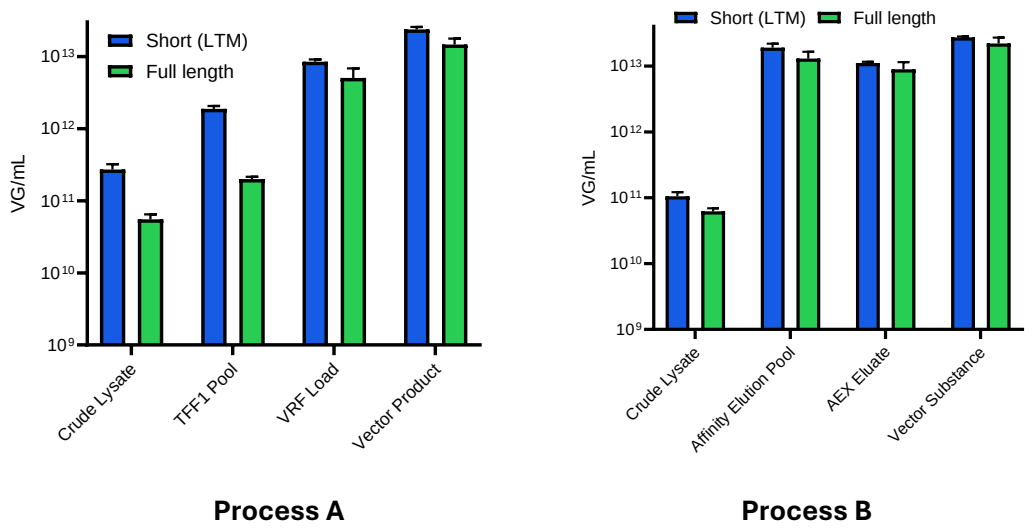

Process A **Process B**

Fig. 5. Short-region (LTM) and full-length quantification of samples from two different processes. The data are an average ± S.D. from 2 - 4 independent measurements (each with two technical replicates) from the indicated manufacturing processes.

		Short Region (LTM)		Full-Length	
		Average	Linearity CV	Average	Linearity CV
Process A	Crude Lysate	2.71E+11	15.3%	5.53E+10	12.3%
	TFF1 Pool	1.88E+12	8.2%	1.96E+11	5.5%
	VRF Load	8.49E+12	6.2%	5.05E+12	29.3%
	Vector Product	2.37E+12	6.8%	1.47E+13	14.3%
Process B	Crude Lysate	1.05E+11	13.5%	6.23E+10	8.1%
	Affinity Elution Pool	1.90E+13	12.0%	1.30E+13	22.1%
	AEX Eluate	1.11E+13	3.4%	9.34E+12	23.4%
	Vector Substance	2.72E+13	2.6%	2.20E+13	18.8%

Table 2: Quantification of viral genome titer by measuring a short region (LTM) of interest or full-length and their linearity CVs. Linearity CV is calculated based on the average back-calculated measurements of the same sample at different dilutions. At each dilution, technical duplicates were measured.

Quantification of the proportion of full-length transgene containing AAV particles

The quantification from the short 3'-ITR-adjacent region measures all molecules that are ≥ 0.12 kb and includes the titers of all 5' or "left" region truncations - what we'll call 5' deletions, or Δ5' molecules - as well as the full-length transgene. We thus define this populations as **L**eft **T**runcations and full-length **M**olecules Titer (LTM), as depicted in **Fig. 3**. Though we didn't do it in this study, a mirrored scenario can be adopted by using a short 5'-adjacent primer/probe set to measure 3' or "right" region truncations; this would measure what we'll call 3' deletions, or Δ3' molecules, as well as the full-length transgene, with this overall population thus defined as **R**ight **T**runcations and full-length **M**olecules Titer (RTM). In contrast to the short probes which capture both fragment and full species, the full-length probes can *only* measure the full-length transgene species (FL).

If one assumes that at least one free ITR is required for packaging and by association that the only packaged partials are those that result from incomplete transcription of the gene of interest after initiation at the ends of the transgene by ITR self-priming, then the total partial fragment count would be LTM + RTM – FL. Thus, the proportion of the full-length species over all packaged molecules (%FL) can be calculated as % FL = FL / (LTM + RTM – FL) x 100. However, it is well established that there exists a population which has both 5' and 3' truncations – what we'll term Δ5'3' or **B**ilaterally **T**runcated **M**olecules (BTMs). Quantification of BTMs requires alternative approaches and is out of scope for this study.

In our study, we have measured the LTM and FL values for two manufacturing processes. Quantitation of just the LTM was chosen out of simplicity to perform the proof-of-concept experiment. As noted, a more complete approach would be to also quantitate RTM, as well as other significant populations (e.g. BTMs). In addition to being able to establish a comprehensive % FL, the quantifications of individual species allow us to elucidate the relative contributions of these species to product quality and conceptualize tailored interventions. For example, RTM and LTM should not be presumed symmetrical in abundance, impact, or specific approach to reduce. Regardless, evaluating "true" fulls as a percentage of either total packaged species or any desired sub-population of packaged species differs from the typical measures of "% full" and "% partial", which presents genetic populations relative to total capsids emphasizing the role of empties. Instead, we spotlight the genetic species relative to each other, emphasizing the role of content, and specifically, truncations.

As an example, we found it potentially instructive to represent the ratio of FL to just LTM. The estimate of FL population as a function of the total measured 5' partial and FL genomes can be calculated as % F_{LTM} = FL/LTM*100. To characterize the manufacturing process, we evaluate %F_{LTM} across the two manufacturing runs shown in **Fig. 6.** The error bars in **Fig. 6** are determined by propagating the uncertainties with both FL and LTM measurement. We can see Process B yields a greater relative proportion of true full-length transgene containing capsids out of the bioreactor. Although not statistically significant, there seems to be some partial clearance from the AEX step in Process B, indicated by the increase of %F_{LTM} in **Fig. 6.**

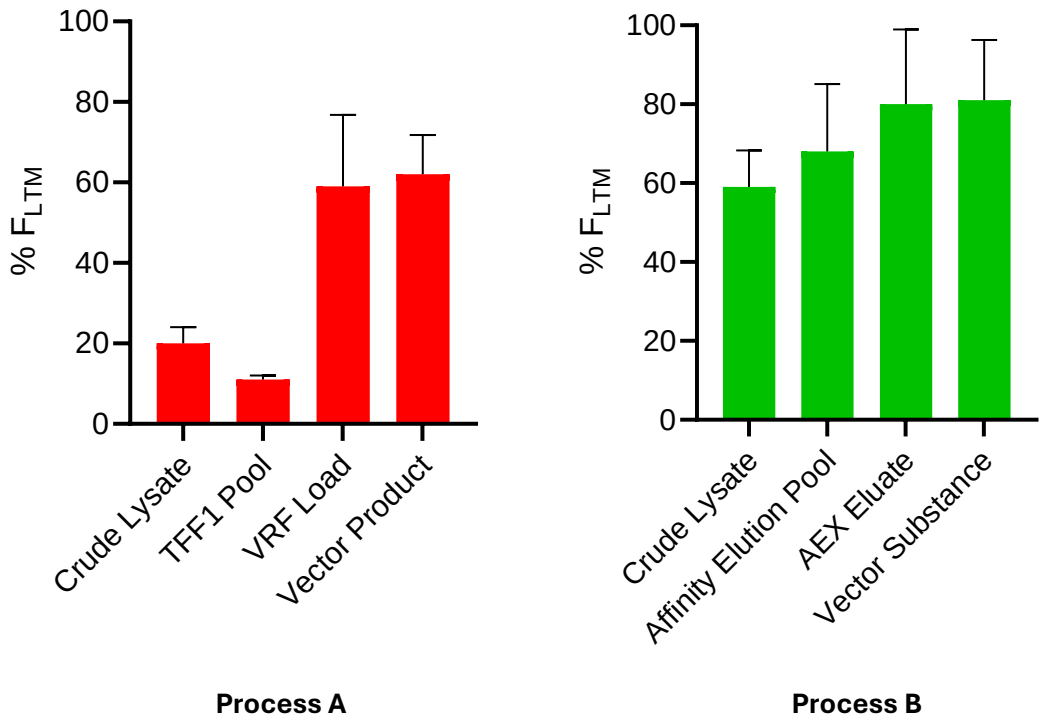

Fig. 6. Comparison of full-length proportion across key manufacturing steps in two different processes. % F_{LTM} was calculated from the ratio of the averaged titers of the full-length (FL) molecules and LTM. The error bars are determined by propagating the uncertainties of FL and LTM measurements.

Effects of TFF on viral genome titers

To derive the effects of post-clarification TFF (TFF1), we calculated the %F_{LTM} from the quantification of the short and the full-length regions. We see that in Process A, where TFF1 was used as a purification process, %F_{LTM} decreased by from ~20% to ~11%. The measurement from the short region (LTM) indicated that there was a 7-fold increase in titer due to concentrating the crude lysates with TFF, while the full-length measurement indicated a 3.5-fold increase.

This implies that during the TFF1 process, the AAV capsids bearing partial genomes are preferentially enriched in comparison to the full-length species. This is believed unlikely, with several possible alternative causes of this phenomena.

To rule out the measurement inaccuracy due to matrix interference, three dilutions of each sample are measured. Typically, when matrix effects are indeed involved, there would be a discrepancy between measurements from the different dilutions, i.e., more concentrated samples would suffer from greater matrix interference and increasing the dilution factor would mitigate interference. **Table 2** outlines the CVs between different dilutions. The low linearity CVs across the TFF1 sample dilutions, both for the short and the full-length probes, indicate that there was minimum matrix interference, or otherwise the interfering element was refractory to our dilutions. We do note

that the dilution required to measure the short region (LTM) was ~30-fold greater than that required to measure the full-length species.

The manufacturing process included the use of a nuclease which, if substantially enriched at TFF1 pooled stage, could introduce the loss of genetic materials. However, the sample preparation step ensures that there are no active nucleases. We came to this conclusion by spiking in plasmid DNA to the TFF1 matrix, either before or after nuclease inactivation. The result indicated that: (i) before the sample preparation, there was significant active nuclease in the matrix to eliminate the spiked-in DNA, and (ii) the proteinase K treatment, which is part of the sample preparation, adequately inactivated the nuclease as confirmed by agarose gel electrophoresis (not shown).

Some other possible causes of this may include the generation of nuclease-resistant unpackaged vector-related genomic material e.g. as chromatin heterocomplexes, or genome ejection from capsids during processing, though neither has been further investigated. While the precise phenomenon has not been clarified, we note that this novel quantitation approach does suggest a possible process-related change in the underlying milieu of material during manufacturing Process A that was not otherwise flagged through traditional analytical methods.

Evaluating %F_{LTM} across the manufacturing processes

In both processes, %F_{LTM} increased after chromatographic operations (**Fig. 6**). This suggests a relationship between %F_{LTM} and bulk purity. We generally see significant amounts of unpackaged nucleic acids (e.g. hcDNA, pDNA) in the crude cell lysate after harvest, and when TFF1 operations are employed, these impurities are further concentrated. For these two processes, only after chromatography do we see appreciable reductions (often BLOQ) of free nucleic acid impurities. This provides further suggestion that even after the nuclease treatment, it is likely that short truncated nucleic acids remain resistant in the crude matrix, and that the changes in %F_{LTM} prior to chromatographic purification are likely picking up those nuclease resistant impurities in the matrix and not changes to the actual vector-packaged material.

By extension, this suggests that any method that uses a small region as a surrogate of the full-length transgene would also pickup – though not distinguish – those impurities. Thus, one may inaccurately quantify the therapeutic AAV populations – picking up those changes in short species but considering them as full length—especially in the crude-matrix background. Ultimately, these traditional tittering methods may not only make it challenging to understand recoveries across earlier downstream operations, but they may lead to scenarios where upstream process optimization leveraging analytical readouts of crude material are biased to enrich partial species instead of the full-length region. This emphasizes the need for quantifying true full-length containing AAV particles in crude matrices to avoid such an optimization bias.

Comparison of Orthogonal Methods

There is no single standard measure of AAV titer or assessment of packaged content. **Table 3**. is a non-exhaustive list of some common approaches. We chose to evaluate 4 samples from the Process B lot: crude harvest, affinity chromatography elution pool, anion exchange chromatography elution pool, and vector substance. We evaluated them across four methods, where possible – ITR2 qPCR, NanoMosaic, Stunner, and Refeyn. qPCR and NanoMosaic are both molecular methods leveraging primer extension and probing, with the qPCR method probing off the (AAV2) ITRs and NanoMosaic utilizing the method as previously described.

Method	Basic Principle
qPCR/ddPCR	Amplifies and quantifies AAV genomes using specific primers.
ELISA	Uses antibodies to detect and quantify AAV capsid proteins.
UV Spectrophotometry	Measures absorbance at 260/280 nm to estimate nucleic acid and protein content.
Dot Blot Assay	Hybridizes labeled probes to AAV genomes immobilized on a membrane.
Infectious Titer	Measures the number of transducing units (functional AAV particles) via cell transduction assays.
Flow Cytometry	Detects fluorescent reporter expression in transduced cells.
HPLC/UPLC	Separates and quantifies AAV particles based on physical and compositional properties. E.g. SEC-MALS, RP-HPLC, IEX-HPLC, AFFINITY-HPLC
Cryo Transmission Electron Microscopy (TEM)	Visualizes and counts AAV particles directly. Can provide titer as well as distribution of packaged species.
AUC (Analytical Ultracentrifugation)	Separates AAV particles based on size and density; quantifies empty, partial and full species.
Western Blot	Detects AAV capsid proteins using antibodies.
NanoFlow Particle Analysis (NTA)	Measures particle size and concentration through image-based assessment of diffusion coefficient based on Brownian motion.
Stunner (Unchained labs)	Combination of UV Vis for protein and nucleic acid detection, and Dynamic Light Scattering for assessment of diffusion coefficient through intensity change of scattered light based on Brownian motion.
Mass Photometry (Refeyn)	Quantifies empty, partial, and full populations based on photometric measurement of molecular mass
Nanoneedle technology (NanoMosaic)	Amplifies and quantifies full-length and partial AAV genomes using specific primers and solid-state reporter-free detection
Next Generation Sequencing	Semi-quantitative method to analyze vector genome purity and sequence variants

Table 3: Selection of common tools for AAV quantification and population assessment.

Stunner and Refeyn are biophysical methods, the former based on a combination of UV detection and dynamic light scattering, the latter on a technique known as mass photometry. We leveraged qPCR, Stunner, and NanoMosaic to assess titer, and we used both NanoMosaic and Refeyn to assess ratios of various species (**Table 4**.)

Unsurprisingly, we found that all systems reported different values for titer. For purified samples the values are correlated; that is, while the actual reported values are different for a given sample across the different analytical tools, the fold changes between samples (e.g. where unit operations may lead to an increase or decrease in titer) are reasonably similar. The crude lysate sample was an outlier, with NanoMosaic indicating a comparatively lower titer than qPCR, versus all other samples wherein the NanoMosaic generated titer was higher.

Refeyn was used to bucket species broadly into "empties", "partials", and "fulls". We previously defined %FL = FL/(LTM + RTM – FL) as a relevant measure for NanoMosaic describing fulls as a percentage of total packaged right-and-left species. The closest equivalent measure for Refeyn is the ratio of fulls to the sum of partials and fulls, which we've represented as $\%FL_{RFN.}$ Since in this initial investigation we only measured LTMs using NanoMosaic, we do not have the data to directly compare Refeyn to NanoMosaic. However, to demonstrate the concept, if we allow the assumption – previously noted as tenuous – of a symmetrical and even distribution of LTM and other truncated species, we can calculate %FL* = FL/((2*LTM) – FL). Interestingly, if entirely speculative, %FL* and $\%FL_{RFN}$ are in the same ballpark. Notably, when looking at $\%F_{LTM}$ (and at %FL* despite the assumptions) whereas Refeyn shows no substantial change in relative percentages of full species across the three matrices evaluated, NanoMosaic suggests a substantial decrease in partials content across the anion exchange step, which, interestingly, is the only downstream unit operation designed to modulate packaged species (enriching for fulls). Specifically, when looking at $\%F_{LTM}$, we see an increase from 68% to 84% across AEX (**Table 4; Fig. 6)**. More work is necessary to better understand these results.

Samples	qPCR	NanoMosaic	Stunner	Refeyn %F_REF	NanoMosaic %FL*	NanoMosaic %F_LTM
Crude Lysate	1.47e11	5.53e10	-	-	11%	20%
Affinity Elution	3.64E+12	1.30E+13	-	73%	52%	68%
AEX Elution	1.90E+12	9.34E+12	3.36E+12	79%	73%	84%
Vector Substance	5.47E+12	2.20E+13	8.80E+12	78%	68%	81%

Table 4. Orthogonal testing of Process B samples measured with qPCR, NanoMosaic, Stunner and Refeyn platforms. Titer values are reported as VG/mL.

Viral genome quantification based on ITR-probes requires caution in selecting standards and interpreting the data.

Complications of the ITR structure

Crucial components of the AAV genome, the ITRs are located at each end of the genome, playing a key role in the virus's life cycle, its manufacture and its utility in gene therapy. The commonly used ITRs in AAV gene therapy are from the AAV2 serotype. AAV2 ITRs are particularly well-studied and recognized for their stability and efficiency in transgene expression, making them the standard choice for many AAV-based vectors. Their structure aids in second-strand synthesis, packaging, and the formation of a circular episome, allowing long-term expression of the delivered therapeutic gene in target cells.

Due to their inherent ubiquity in rAAV sequences, ITRs have been used as a convenient universal method to determine transgene titers using qPCR or ddPCR. However, the complicated structure of the ITR poses the following challenges in measurement.

ITR secondary structure

The primary structure of ITRs lead to their ability to replicate and package viral genomes. Due to its role in packaging, ITRs can be packaged containing only minimal vector genome components. Additionally, ITRs form a stable hairpin structure due to their palindromic sequences making these regions susceptible to high degrees of truncation and snapback events. This secondary structure can also resist or can quickly fold back on itself after denaturation during the PCR process. Due to the tight folding, the ITRs can prevent the binding of DNA polymerase and primers, resulting in reduced amplification efficiency [8].

Self-priming

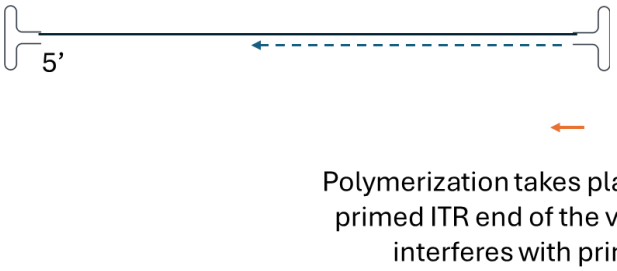

Fig 7. ITR self-priming effect. Schematic to show polymerization from the ITR self-primed

The ITR, when folded back on itself, presents an available double stranded DNA 3’- end which acts a primer [9]. When PCR ensues, the self-primed hairpin can be polymerized instead of the desired sequence from the intended target primers (**Fig. 7**). This can lead to the formation of self-complementary viral genome molecules that are refractory to PCR, thereby further complicating the analysis and accurate quantification from the ITRs.

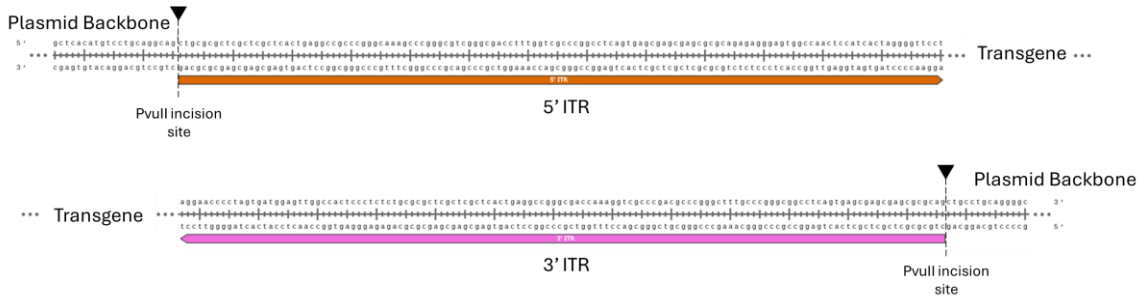

Fig 8. Generation of ITR-to-ITR plasmid DNA standard. The above schematic shows an example of a transgene containing plasmid where the PvuII restriction site bookends the transgene sequence. Thus, restriction digestion with PvuII will accurately incise the plasmid, releasing the backbone sequence and the transgene sequence from the 5' ITR to the 3' ITR, which mimics the packaged rAAV DNA.

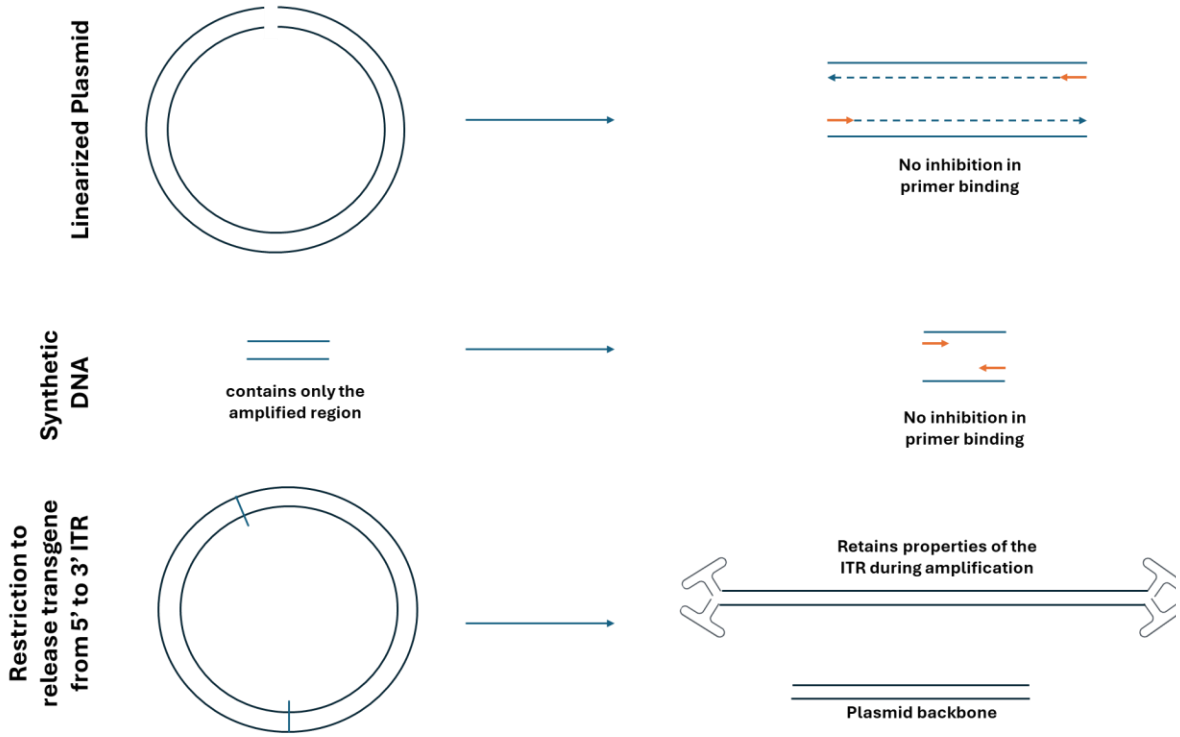

Fig. 9. Difference between different standards used for ITR-based quantification. The different standards that are used for measuring the ITR-specific region and method to generate them are indicated.

Bias in quantification when different standards are used

To quantify ITRs more accurately, if using plasmid, the plasmid containing the transgene should be restriction digested in a manner that preserves the ITRs at both ends (**Figs. 8, 9)**. In this situation, each strand of pDNA standard will have ITRs at either end as well as the potential for formation of an approximation of their native structure during amplification (**Fig. 9**). The preservation of some structure will present more similar bias in ITR measurement as would be presented in the sample thereby more accurately quantifying the sample. This would be the most conservative approach for measuring the ITRs with pDNA though it has certain weaknesses as discussed below (**Fig. 9**). There are also cases where a linearized plasmid, or only the region to be amplified (synthetic DNA) is used as the standard for quantification, as illustrated in **Fig. 9**. However, in these situations, the standards may lack all or enough of the ITR sequences to lack any potential for configurations resembling the secondary structure of the ITRs and thus have a higher amplification efficiency than when the standard has a preserved ITR structure (**Fig. 10**). This could lead to under-quantification of the sample.

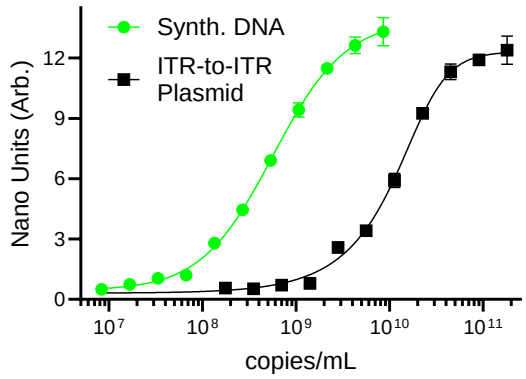

Fig. 10. Calibration curve using synthetic DNA or ITR-to-ITR restriction digested plasmid using ITR region specific probes. There is a 10-fold difference between the two standards.

Caution in the interpretation of ITR results

When using the plasmid cut from one ITR end to the other, since the standard has two ITRs per molecule, the final estimated sample quantification is under the assumption that each VG molecule measured from the sample has two ITRs (**Figs. 8, 9**). But partial molecules may have only one ITR, either on the 5' or the 3' end. Thus, the actual titers can be up to 2-fold greater than the measured value (2-fold greater would be in the case that each VG molecule has only one ITR). Moreover, if the partial genome only has the 5' ITR, then it would lack the self-primed 3'-end, and thus will not have compromised amplification efficiency from self-priming. Thus, for all these unknowns, the ITR-based VG quantification should be interpreted with caution, perhaps even only qualitatively. Additionally, due to the propensity for many truncated/partial genomes to be created during rAAV production, it's highly likely that single-ITR containing genetic species of all different sizes are misrepresented as complete genomes when measured by the ITR-assay. Both characteristics thus make quantification of full-length, intact genomes inaccurate via ITR based assays.

Comparison of ITR-based measurement using different methods and standards

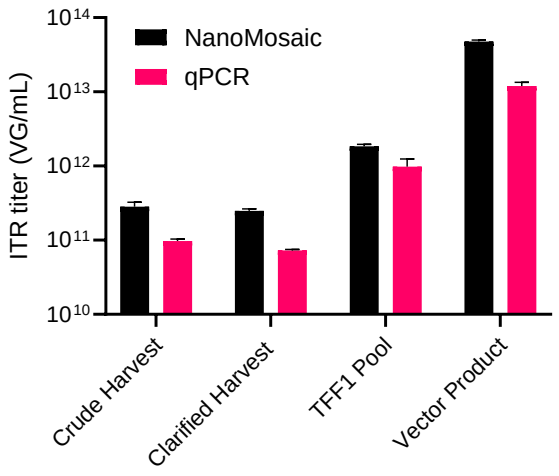

Fig. 11. Comparison of ITR-measurement between nanoneedle method to qPCR. The difference in the titer of the ITR-region when using qPCR and a synthetic DNA standard (N=6), or ITR-to-ITR digested plasmid and the Nanoneedle technology (N=4-6 replicates).

We have previously discussed the unique value propositions of LTM, RTM, and true-full detection inherent to the design of the nanoneedle technology and probe system. We have also highlighted some risks associated with pure ITR-based quantification. Nonetheless, we were curious to see how the nanoneedle system performed when simply using it for classic ITR-based quantification. It is still commonplace for ITR-qPCR assays to be run, and we wanted to understand how the nanoneedle technology performed in comparison (for example, if a researcher wanted to utilize a nanoneedle instrument for reasons such as throughput, convenience, bridging, etc., while running a low-dimensionality ITR quantification). We thus compared the nanoneedle technology to ITR-qPCR using a different lot of Process A material. In our study we quantified samples using identically designed ITR probes by both qPCR and nanoneedle. For nanoneedle we used the ITR-to-ITR restriction digested plasmid as the standard, while for qPCR we used synthetic linearized dsDNA as standard. We observe that the quantifications were highly correlated. The values were generally lower (as much as 0.5 log) when using qPCR with the synthetic dsDNA as standard compared to nanoneedles with restriction digested plasmid. We cannot definitively attribute the source of the offset – whether method, or standard as per **Fig. 10** – as we did not evaluate the cross comparison. We expect the offset is driven by a combination of both. Regardless, these data demonstrate how titer based on ITR can be highly method specific.

Conclusions

In this whitepaper, we present the performance of nanoneedle technology in quantification of AAV subpopulations in different sample matrices across different manufacturing processes. As demonstrated in two different manufacturing processes, the quantifications of the full-length transgene species can be significantly different from short partial transgenes, suggesting significant limitations with the typical approach of using short-probed regions as quantitative surrogates for full transgenes.

The viral genome assay is straightforward to set up by positioning two probes at any location of the viral genome to specifically quantify the DNA content at different sizes. With calibration-curve CVs of 2.8% and 2.6% presented in the above cases, the assay is capable of consistent performance. While not presented here, there are no physical limitations to scaling this workflow to any SBS-compatible plate, including the use of automation in 96, 384 or 1536-well nanoplate formats.

Small sample volumes (2 µL) make the process very attractive, and sample prep is comparable if slightly more complicated than typical PCR-based workflows. Compatibility of the method with the range of matrices from crude lysate through vector substance enables quantification of true full-length vector throughout the process, and, importantly, upstream optimization against the production of true full-length vector. However, like most methods, some caution must be applied with highly crude matrices; in this case, quantitative interpretation of partials may be susceptible to challenge from crude matrices.

Realization of the full potential of AAV for gene and cell therapy requires continuous improvement of manufacturing processes and product quality. Novel tools will be critical to the increased breadth and depth of insight required to achieve this. We see nanoneedle technology as a highly promising option for achieving these goals.

Contributions

Project Design/Conceptualization: D. Hurwit, D. Steinhauff, A. Garg, Q. Quan

Experimental Design/Experimentation: A. Garg, T. Raz, Q. Quan, D. Hurwit, D. Steinhauff

Authoring: D. Hurwit, A. Garg, T. Raz, Q. Quan, D. Steinhauff,

References

1 Wang D, Tai PWL, Gao G. Adeno-associated virus vector as a platform for gene therapy delivery. Nat Rev Drug Discov. 2019; **18**. doi:10.1038/s41573-019-0012-9.

2 Jiang Z, Dalby PA. Challenges in scaling up AAV-based gene therapy manufacturing. Trends Biotechnol. 2023; **41**. doi:10.1016/j.tibtech.2023.04.002.

3 Halbert CL, Allen JM, Miller AD. Adeno-Associated Virus Type 6 (AAV6) Vectors Mediate Efficient Transduction of Airway Epithelial Cells in Mouse Lungs Compared to That of AAV2 Vectors. *J Virol* 2001; **75**. doi:10.1128/jvi.75.14.6615-6624.2001.

4 Verdera HC, Kuranda K, Mingozzi F. AAV Vector Immunogenicity in Humans: A Long Journey to Successful Gene Transfer. Molecular Therapy. 2020; **28**. doi:10.1016/j.ymthe.2019.12.010.

5 Zeltner N, Kohlbrenner E, Clément N, Weber T, Linden RM. Near-perfect infectivity of wild-type AAV as benchmark for infectivity of recombinant AAV vectors. *Gene Ther* 2010; **17**. doi:10.1038/gt.2010.27.

6 McColl-Carboni A, Dollive S, Laughlin S, Lushi R, MacArthur M, Zhou S *et al*. Analytical characterization of full, intermediate, and empty AAV capsids. *Gene Ther* 2024; **31**. doi:10.1038/s41434-024-00444-2.

7 Tam Tran N, WL Tai P. Profiling AAV vector heterogeneity & contaminants using next-generation sequencing methods. *Cell Gene Ther Insights* 2024; **09**. doi:10.18609/cgti.2023.206.

8 Liu Z, Zhao C, Zhao G, Xiong S, Ma Y, Zheng M. Disruptors, a new class of oligonucleotide reagents, significantly improved PCR performance on templates containing stable intramolecular secondary structures. *Anal Biochem* 2021; **624**. doi:10.1016/j.ab.2021.114169.

9 Brister JR, Muzyczka N. Mechanism of Rep-Mediated Adeno-Associated Virus Origin Nicking. *J Virol* 2000; **74**. doi:10.1128/jvi.74.17.7762-7771.2000.